Geological and Structural Interpretation of Ado-Ekiti Southwest and its Adjoining Areas Using Aeromagnetic Data*

Ayodeji Jayeoba[1] and Dare Odumade[2]

Search and Discovery Article #30407 (2015)
Posted July 13, 2015

*Adapted from extended abstract prepared in conjunction with oral presentation given at Pacific Section AAPG, SEG and SEPM Joint Technical Conference, Oxnard, California, May 3-5, 2015.

[1]Department of Geology, University of Ibadan, Ibadan, Nigeria
[2]Nigerian Mining and Geosciences Society, Zawan, Nigeria (dare.odumade@yahoo.com)

Abstract

Airborne magnetic datasets over Ado-Ekiti Southwest (sheet 244) was processed to interpret the geology and estimate the depth to basement of magnetic sources in the area in order to evaluate and deduce the basement topography, delineating structural lineaments, and their trends using the aeromagnetic geophysical method.

Aeromagnetic dataset were collected, filtered, inverted, and enhanced using appropriate software packages and subsequently employed to generate a model of the subsurface basement topography. The data processing steps involved were Butterworth filtering, reduction to the equator, analytic signal, upward continuation, Tilt angle derivative, Average power spectrum, Euler deconvolution, and Window Euler solution.

The magnetic intensity from Butterwort ranges from -171.647 to 188.405 nT; Reduction to the Equator varies from -162.5 to 194.1 nT; upward continuation at 4 km ranges from 7.6 to 91.7 nT and analytical signal varies from 0.007 to 0.564 nT. The magnetic intensity distribution was found to depend on the size, depth of burial, and the thickness of low susceptibility superficial material overlying the magnetite rich crystalline rocks. Tilt angle derivative revealed the presence of fold, shearing, and lineaments with its orientations. Lineament analysis using the rose diagram showed that the area is dominated by NNE-SSW trend. Window Euler solution varies from 0.132 km to 2.23 km with the percentage variation in the depth estimation ranging from 5.56% at shallow depth to 0.90% at deeper depth. The average radial power analysis delineated shallow sources ranging from 0.36 km - 0.50 km with 95.2 nT - 134.9 nT magnetic intensity and deeper sources ranging from 0.88 – 1.35 km with magnetic intensity -37.4 nT to -162.5 nT.

Maps of upward continuation, analytical signal, tilt derivative, average power spectrum, Window Euler solution, and Rose diagram revealed the basement topography including structural lineaments with its orientations and the depth to the magnetic sources of the study area.

Introduction

Aeromagnetic survey maps the variation in geomagnetic field, which occurs due to the changes in the percentage of magnetite in rock. It reflects the variation in the distribution and type of magnetic minerals in the subsurface. Magnetic minerals can be mapped from the surface to greater depth in crustal rocks depending on dimension, shape, and the magnetic property of the rock. Sedimentary formations do not usually have appreciable magnetic properties, this is because of the minute contribution of detrital remnant magnetism while igneous and metamorphic rocks exhibit greater variations and become useful in exploring bedrock geology.

Ado-Ekiti Southwest and its adjoining areas has witnessed several geophysical investigations such as VLF (very low frequency) and VES (vertical electrical sounding) studies, borehole logging (lithologic and geophysical), electrical resistivity probing, electromagnetic surveys, surface mapping among others to determine its groundwater potential and evaluate its geologic and economic values but little has been done in the area of magnetic mineral prospecting or exploration. Therefore, the need for a cost effective, rapid result, risk reduction and faster technique like aeromagnetic method which can give quick and reliable information about the subsurface basement structures, subsurface lithology, trend, depth to magnetic source, and structural features of large and inaccessible areas is necessary hence, this study.

The study area is located within the basement complex region of Nigeria and indicators that have been found useful in mineral exploration includes faults, fractures (lineaments), arched, or domed structures in addition to oxidized and hydrothermally altered areas (Peterson et al., 1976), and the application of aeromagnetic methods amplifies the recognition of the difference in depths of magnetic sources, structures like faults, dike, lineaments, and layered magnetic susceptibility given in the variability of complexes. This report is supposed to serve as a guide for geologically related decision making prior to exploration and constructions. The study area is located between longitudes 5°00′ E and 5°15′ E and latitudes 7°30′ N and 7°45′ N, covering an area of 1,471.5 $km^{2.}$

Geological Setting

The study area is part of the basement complex of southwestern Nigeria and is Archean to early Proterozoic in age as described by Talabi (2013). More so, Oversby (1975) and Olanrewaju (1981) indicated that the study area is composed of migmatite-gneiss-quartzite complex with little supra-crustal rock relics. The basement complex of Nigeria is zoned in the western part of the Pan-African shield as described by McMurry (1976) and Ball (1980), occurring in the mobile zone of the Pan-African reactivation area between the West-African craton to the west and the Congo craton to the southeast.

The following distinguishable lithologies can be identified from the geologic map of the study area (Figure 1) and they are; quartzite, migmatite, schist with pegmatite intrusion, biotite rich granites, charnokitic rocks, and quartz veins.

Aeromagnetic Data and Analysis

Data Acquisition

As part of a nationwide high resolution airborne geophysical survey aimed at assisting and promoting mineral exploration in Nigeria, aeromagnetic data was acquired between 2003 and 2009 by Fugro Airborne Survey Limited for the Nigerian Geological Survey Agency (NGSA) (MMSD, 2010). The data was collected systematically by dividing the country into geological blocks with dissimilar measurement parameters for each block with the eventual production of an aeromagnetic map for the whole country.

The Scintrex CS3 Cesium Vapor magnetometer was used and it is an optically pumped cesium vapor magnetometer used for scalar measurement of the Earth's magnetic field. It can be used in a variety of applications such as airborne, satellite, ground magnetometry, or gradiometry. It is highly sensitive and measures in the range of pT (1 pT = 0.001 nT) in a measuring bandwidth of 1 Hz and this sensitivity does not deteriorate as the measured ambient field decreases. It measures between 15,000 nT and 100,000 nT. The sensor head has an electrode-less discharge lamp (containing cesium vapor) and absorption cell. Electrical heaters bring the lamp and the cell to optimum operating temperatures with control and driving circuits located in the electronics console. Heating currents are supplied to the sensor head through the interconnecting cable.

The area under study, Ado-Ekiti Southwest and its environs designated as Sheet 244; is part of Block B and was surveyed in Phase 1 of the project. The survey was carried out by fixed wing (Cessna) aircraft covering a total of 235,000 line kilometers with a flight spacing of 200 meters and a terrain clearance of 80 meters, The flight direction was NW-SE with tie-line spacing of 200 meters and tie-line direction of NE-SW.

A recording interval of 0.1 secs and a grid mesh size of 50 meters were applied in the World Geodetic System of 1984 (WGS84) within UTM Zone 36S and with the Clark 1880/Arc 1960 coordinate system.

Data Processing

The data is that of total field and is in a gridded form as a total magnetic intensity (TMI) map (see Figure 2). This method fits minimum curvature curves (which is the smoothest possible surface that would fit the given data values) to data point using method described by Briggs (1974).

Data Filtering

Butterworth filter which is a low-pass filter was applied in accordance with I.G.R.F reduction technique. A low-pass filter is a filter that passes low-frequency signals and attenuates (reduces the amplitude of) signals with frequencies higher than the cut off frequency. The actual amount of attenuation for each frequency varies depending on specific filter design. Low-pass Butterworth filter was applied to the total magnetic intensity data to remove regional effects. An ideal low-pass filter completely eliminates all frequencies above the cut off frequency while

passing those below unchanged. The residual magnetic intensity (RMI) data were processed using Butterworth low pass filtering technique to increase the signal to noise ratio and to remove all high frequency events which are representative of cultural, processing, or other forms of noise or error in the data and then subjected to further processing.

Downward continuation, a low cut and optimum filter were also applied to enhance responses emanating from shallower sources; this was achieved by moving the detector closer to the source. The principle is such that, short wavelength signals are likely to originate from shallow sources, hence signals originating from a particular depth source could be selected based on wavelength. A plot of radially averaged power spectrum was used to determine the wavenumbers corresponding to shallower sources; consequently, everything below the wavenumber corresponding to the depth of interest was treated as noise and silenced using low cut filter in line with (Osinowo and Olayinka, 2013).

Upward continuation filtering were subsequently applied to filtered data and transforms the data into that which would have been measured at a higher altitude than at which it was actually measured. It is useful for smoothing data, among other things. Since, this filter is considered a 'clean' filter because it produces no side effect that may require the application of other filter or process to correct. In this case, it is often used to remove or minimize the effects of shallow sources and noise in grids.

Reduction to Magnetic Equator

To produce anomalies depends on the inclination and declination of the body's magnetization, inclination, and declination of the local earth's field and orientation of the body with respect to the magnetic north (Baranov, 1957), it is usually necessary to perform a standard phase shift operation known as Reduction-to-Pole (RTP) on the observed magnetic field. In magnetic equatorial regions where inclination is less than 15°, RTP is generally unstable and cannot be derived because such data introduces north – south alignment of the anomalies into the data, thereby making the data unstable. A similar effect is seen when a magnetic field is Reduced-to-Equator (RTE) instead of to the pole depending on the latitudinal position of the study area. Once the field has been reduced to the equator, the regional magnetic field will be horizontal and most of the source magnetizations will be horizontal.

For the vital purpose of accurate positioning, the total magnetic intensity map was reduced to equator prior further processing to correct for effect of latitude and to make the magnetic anomalies to be symmetrically centered over their corresponding sources because the study area is closer to the equator. In this report, RTE was applied to the filtered map with -10.724^0 and -4.880^0 representing the inclination and declination respectively of the geomagnetic field parameters of the central location of the study area as seen in Figure 3 and was used for the reduction. The airborne magnetic datasets were further processed with respect to Figure 4.

Method

With the main aim of analysing, detecting, and interpreting the available aeromagnetic map of the study area to identify the possible tectonic setting as well as subsurface structures, Mineralized zones and propose a new geological map of the area under study, the approach used by Feumoe et al., (2012) was adopted. This method includes the use of the FVD method to detect linear structures, the pseudo-gravity to delineate

crustal magnetic sources while the Euler deconvolution and the average power spectrum are used to determine depths of deep and shallow magnetic body sources.

First Vertical Derivatives (FVD)

Derivative filtering techniques are used to sharpen the edges of magnetic anomalies and better locate their positions. The reduced to the equator total magnetic intensity map contains all the anomalies representative of both shallow and deep sources. Therefore, derivative filtering techniques are to be applied on it so as to suppress unwanted sources (and enhance some) or to sharpen the edges of the anomalies. Vertical derivatives enhancement sharpens up anomalies over bodies and tends to reduce anomaly complexity and allow clearer imaging of the causative structures. Vertical derivatives map/profile enhance the lineament and anomalies owing to their short wavelength character.

When the first vertical derivatives is applied on the magnetic data, it enhances shallow wavelength features, that are results of near surface structures, and suppresses long wavelength ones (deeper sources) thereby provide a better and clearer picture of the subsurface.

The first vertical derivatives filter was applied to the reduced to equator, total magnetic intensity data to enhance local anomalies obscured by the broader regional trend. In this case, it amplifies short wavelength components of the field and de-emphasizing the long wavelength components thereby giving clearer contrast between the geologic units.

The tilt derivative in Figure 5a and Figure 5b, amplifies lineaments, which are structural deformations that are related to faults, joints, and arched zones or even geological contacts. Magnetic minerals are mainly concentrated along or aligned with some structures or sedimentary features such as faults or channels. The tilt map (Figure 5) has the parallel and sub parallel lineaments picked out.

Pseudo-gravity

According to Pratt and Shi (2004), the pseudo-gravity transformation is one of many possible FFT techniques that can be applied to aeromagnetic data. It enhances the anomalies associated with deep magnetic sources at the expense of the dominating shallow magnetic sources. This transformation is an excellent interpretation tool for the detection of deep, magnetic igneous plutons and volcanic piles and the transformed data can be modelled using conventional gravity modelling tools. It is a suitable tool for interpreting deep-seated mineral plumbing systems associated with known, shallow mineral occurrences.

The enhanced pseudo-gravity transform is derived from the standard pseudo-gravity transform by removing long wavelength anomalies that are associated with FFT processing properties and deep crustal magnetic sources. Conventional low-pass and upward continuation filters were considered but a modelling approach was adopted to remove the influence of magnetic sources that are beyond the zone of exploration interest. The pseudo-gravity data can be modelled using conventional map modelling and inversion methods, where the density is considered as a pseudo-density defined by the relationship

$$D = kH/\gamma, \qquad 1$$

Where D is the density contrast, k is magnetic susceptibility, H is the total magnetic field intensity, and γ is the universal gravitational constant. This relationship assumes that the magnetization is induced and no remanence is present.

Power Spectrum and Euler Deconvolution

Each wavelength's power unit can be plotted against wavenumber regardless of direction, to produce a power spectrum. In frequency domain, one can prepare and analyse the distribution of short to long wavelength across all measured high to low frequency. The power spectrum can be broken into series of straight lines segments and each segment represents the cumulative response of a discrete assemblage of sources at a given depth. The depth is directly proportional to the slope of the line segment (Spector and Grant, 1970). Potential field may be considered as representing a series of interfering waves of different wavelengths and directions.

The slope of each segment provides information about the depth to the bottom of the magnetic bodies (Kivior and Boyd, 1998). Radially averaged power spectrum of magnetic data according to Blanco-Montenego et al., (2003) is expressed as a function of wavenumber and is related to depth to the bottom of the deepest sources as expressed in equation 2.

$$K_{max} = \frac{\log Zb - \log Zt}{Zb - Zt} \qquad 2$$

Where Zt and Zb are depth to top and depth to bottom of the magnetic sources respectively. K is a function of wavenumber which is expressed in radian per unit distance.

In this study, power spectrum analysis was carried out on aeromagnetic data using Geosoft® Oasis Montaj™ software to identify average depths of source assemblage. This same technique was also adopted to attempt identification of the characteristic depth of the magnetic basement, on a moving window basis, merely by selecting the steepest and therefore straight line segment of the power spectrum, assuming that this part of the spectrum is sourced consistently by basement surface magnetic contrast.

The standard Euler deconvolution method as described by Reid et al., 1990 and Thompson, 1982 obtains its solutions by inverting Euler's homogeneity equation over a window of data at every grid point. As a result, solutions may be generated in areas that are free of anomalies or on the edges of anomalies, even if it is inappropriate to do so. The application of Euler deconvolution has emerged as a powerful tool for direct determination of depth and probable source geometry in magnetic data interpretation (Roy et al., 2000 and Muzala et al., 1999).

Euler derived interpretation is not restricted by any geological preconception and can be used to appraise geological and structural interpretation (Phillisp, Saltus, and Reynolds, 1998). It also requires only a little prior knowledge of the magnetic source geometry and information about the magnetization vector (Barbosa et al., 2000). If a total field (T) measured at a point (X, Y, and Z) has a base level of b and derivatives (dT/dx, dT/dy and dT/dz in the Xi, Yi, and Zi direction), the 3-D form of Euler's equation is defined by Reid et al., (1990) as:

$$XdT/dx + YdT/dy + ZdT/dz + \eta T = X_O dT/dx + Y_O dT/dy + Z_O dT/dz + \eta b \quad (3)$$

$$(x-xo)dT/dX + (y-yo)dT/dY + (z-zo)\, dT/dZ = \eta\,(b - T) \quad (4)$$

Where η is the structural index (SI) defined as the degree of homogeneity of the source body interpreted physically as the attenuation rate with distance. Its value needs to be chosen according to prior knowledge of the source geometry (Table 1), b is the background value of the field while $X_{0,}$ Y_0, and Z_0 is the position of a source whose total field T is detected at any point.

Advantages of this method compared to other classical methods are:

- No particular geologic model is assumed
- Euler equation is insensitive to magnetic inclination, declination, and remanence

In this study, the Euler deconvolution algorithm using Oasis Montaj™ for location and depth determination of causative anomalous bodies from gridded aeromagnetic data was used. The map thus produced shows the locations and the corresponding depth estimation of geologic sources. Also, Extended Euler deconvolution was carried out to determine the depth to the magnetic basement from profiles at estimated level of certainty. This is in line with works of Reid et al., 1990.

Structural Index (η) values 1.0 and 2.0 were used based on the geological models of the source to be individual dikes, sills, and horizontal cylinder as in the case of large plutons respectively (Osinowo and Olayinka, 2013).

The derived solutions were further polished by using the Windowing Technique in order to reduce uncertainty to the barest minimum. This was achieved by constraining the obtained Euler deconvolution solutions to accept maximum % depth of tolerance of 10%, thus depth uncertainty (*dz* in %) greater than 10 % were rejected. Similarly, horizontal uncertainty (*dx* in %) was set to 20 %. This automatically appends mask to those solutions with results that fall out of the specified window.

Minimum window size was used since the maximum width of anomaly expected based on field observation is around 250 m (El Dawi et al., 2004) and this value will ensure that a solution point constitutes a single anomaly point. Generated solutions were windowed to plot only solutions that are within acceptable limit as a measure to further reduce spurious results.

Results and Discussion

Structural Interpretation

The aeromagnetic data was processed in the first vertical derivative filters as well as, for the tilt derivative. The tilt derivative (Figure 5) amplifies lineaments, which are structural deformations that are related to faults, joints, and arched zones or even geological contacts. Magnetic minerals are mainly concentrated along or alligned with some strcutures or sedimentary features such as faults or channels.

Figure 5, displays most structural feature of the area such as the inferred faults, contacts and to some extent the shape of some lithologic contants. Tilt derivative image (Figure 5a and Figure 5b) also show different lineaments and contacts in the area. The basement rocks are seen to be highly faulted and deformed. This deformation and folding was as a result of the pronounced deformation and remobilization that occurred during the Pan-African orogeny about 650-450 million years ago (Odeyemi, 1981). Prominent lithologic contacts observed are; the migmatite-granite (C1, C2, C3) in Figure 5b. Some structural lineaments (faults) e.g. F1, F2, F3, F4, and F5 were delineated by observing the abrupt change between the positive and negative magnetic anomalies.

Figure 6 gives a rough idea of the geological structural control and lithologic deformations in the basement complex of Ado-Ekiti Southwest and its adjoining areas. The portions marked as lineaments and arched structures are of dark straight and angled strokes, indicating low magnetic intensities.

The lineaments (faults) are marked in black ticks while folds and shearing as interpreted by Graham et al., (2014), are marked in arched curves. The orientation and length of the lineament extracted from the Vectorization map (Figure 6) were displayed in a rose diagram to analyse the spatial distribution of lineaments and in order to contribute to the understanding of the directions of the structural control of the study area. The rose diagram (Figure 7) shows trends were NE-SW, NNE-SSW, and NW-SE with minor ENE-WSW, E-W directions. Out of the 67 extracted lineaments, 35% (representing the largest) trends in the NNE-SSW direction with 15% striking in the EW direction. 15% also strikes in the northeast southwest (NE-SW) and another 6 % trending in the north-south (N-S) direction. Most of these trends agreed with previous work carried out in the Benue Trough and parts of the adjoining basement complex of Nigeria by Ajakaiye et al., (1991). According to Dobrin and Savit (1988), lineation in the magnetic contours usually follows regional geology (e.g., intrusive bodies or large faults' strikes) and is thus useful in mapping structural trends. They also stated that well-defined boundaries between zones having appreciably different degrees of magnetic relief often indicate the presence of major basement faults and fractures.

Basement Analysis using Upward Continuation

For proper understanding of the basement complex, structural analysis must be taken into consideration according to (Alexander et. al, 1998). Hence, the need to further process the enhanced Residual Magnetic Intensity map of the study.

This RTE was upwardly continued to 1 km, 2 km, 3 km, and 4 km to accentuate the response from the basement rocks. The most important effects of this filter on the map is that, it makes them smoother and more regional thereby reflects regional basement anomalies. Not much changes were observed in the 1-3 km upward continuations but the 4 km result was more pronounced. In (Figure 8) the positive anomaly of intensity 77.3 nT – 91.7 nT (pink) still appears as a large subrounded anomaly in the central part of the map and extends faintly to the southwest while the negative anomaly of intensity 14.02 nT to -7.6 nT still appears very large in the north-central point extending east of the map. The negative anomaly lies in the area underlain by migmatite rocks in the Igede Ekiti settlement, as well as the southern part of Awo-Ekiti and part of Araramo and Iyin. This is unusual and it is therefore inferred that the negative anomalies must have resulted from the intrusion of hydrothermal fliuds which can deposit less magnetic materials in the fractured rock. The fracture trends northeast-southwest in line with other fractures (lineaments) observed in this area while the positive anomaly in the center of the map rocks extends towards the southwest,

covered by the migmatite complex at Ilawe-Ekiti and Iyin Ekiti and Ado-Ekiti sits in the middle of this entire area. The different rock boundaries cannot be distinguishly mapped out by the upward continuity filter because the same rock unit exhibits both positive and negative magnetic anomalies thus making it difficult to mark out boundaries of different rock units.

Analyitcal Signal

The analytical signal derivative map (Figure 9) accentuate the variation in the magnetization of the magnetic sources in the study area and highlights discontinuities and anomaly texture. Hence, indicates that the linearments are playing host to these shallow sources as observed. The analytical signal map displays the magnetic zone with high intensity of 0.3 nT - 0.6 nT (pink) from north to south and towards the west while regions with low magnetic intensities 0.007 nT (blue) can be seen in the southeast.

Three major magnetic zones i.e. high magnetic anomalous zone are defined as (BM), intermediate magnetic anomalous zone (BQ), and low magnetic anomalous zone (BG) were delineated (Figure 9). The high magnetic signatures at (BM) of the analytical map are the migmatite rocks (Telford et. al., 1990) which were found around the south to north part of the area and trend in the northeast-southwest direction. Lithological contacts portrayed by a sharp magnetic contrast were accentuated; prominent among them were the migmatite-quarzite contact (white line) and the granite-migmatite contact (black line). The granite is acidic, constituting minerals of low magnetic intensities such as quartz when compared to migmatite rocks, which dominates the area.

Merging the enhanced tilt derivative map and the analytical signal map makes noticable the regions in which faults and fractures has been filled with magnetic minerals (Ndougsa-Mbarga, 2011) these areas includes, Igbara-Odo, Erijiyan, Ilawe-Ekiti Environment, and a very large anomaly lies beneath the Igbede Ekiti and Iyin – Ekiti. It can also be deduced from the analytic signal map that these near surface anomalies mainly cover the region occupied by the migmatite-gneiss complex rocks.

The comparative study of the original geological map (Figure 1) and proposed geologic map (Figure 10) of Ado-Ekiti Southwest and its adjoining area showed that structural lineaments are nearly evenly spread across the different rock types and are relative to the positions of the volcanic intrusions and quartz veins just has spotted on the migmatite rock on the original geological map indicating that both maps corresponds. This lineaments are perculiar to basement complex rocks which are of Pre-cambrian age (migmatites, gneisses, and older granites) and this was due to the effect of several tectonic deformations which occurred throughout the Nigerian basements complex.

The arch structures majorly occur on the migmatites and the granitic rocks, thus indicating intense deformation (ductile) when compared with the quarzites and schist with less deformation.

In vectorizing the lineaments into short linear segments, the detection of the contact occurrence density is done as a preamble (Figure 11) to finding where the linear structures intercept or change direction. Historically, these are areas with a high prospect for mineralization. From this the areas of junction with high density can be indicate as seen in the orientation entropy heat map in Figure 12, when the localized junction from Figure 11 are picked/outlined. These high density areas in red are areas favourable for hosting deposits of interest and could be further explored in more detail.

Pseudo-gravity

In order to locate and outline crustal magnetic sources, transformation techniques must be applied. A pseudo-gravity transformation is useful in interpreting magnetic anomalies, not because a mass distribution actually corresponds to the magnetic distribution beneath the magnetic survey but because gravity anomalies are in some ways more instructive and easier to interpret and quantify than magnetic anomalies (Blakely, 1995). When Figure 12 is compared to the psuedo-gravity map in Figure13, the area of high density here is in agreement with the mineralization map (Figure 12) as NE-SW trend in both maps and is emplaced on the migmatite rocks around, the Aramoko-Ekiti area and environs. Thus, the pseudo-gravity map helps deduced a large causative body trending NE-SW with a density of about 0.103 g/cc in susceptibility as seen on the map.

Power Spectrum

Power Spectrum is a 2D function of the energy and wave number and can be used to identify average depth of source assemblages (Spector and Grant, 1970). Figure 14 is the result of the computed radial power spectrum and depths to top of the magnetic sources around Ado-Ekiti Southwest and its adjoining areas can be calculated from this. Slope method used was the Peter's half-slope method as it's widely used especially for aeromagnetic interpretations. These graphical techniques use the sloping flanks of profiles to estimate depth to magnetic sources or depth to basements (thickness of sediments) in sedimentary basins (Nettleton, 1971; Telford et al., 1990).

The result shows that the depth to the top of the deeper magnetic source (outlined by slope 3) varies from 0.88 – 1.35 km with low magnetic intensity ranging from -37.4 nT to -162.5 nT, characterized by longer wavelength anomaly while most of the shallower sources (slope 2) varies from 0.36 km - 0.50 km with anomaly of high magnetic intensity values varying from 95.2 nT - 134.9 nT characterized by short wavelength anomaly.

The shallower sources probably depicted depths to Precambrian basement or near surface igneous intrusive rocks (such as migmatite complex and granite) with remnant magnetism. The deeper sources were characterized by high negative anomaly values having longer wavelength and depicted basic intrusive rock at depth or intruding dike at depth.

Euler Deconvolution

The Euler solution was applied in determining the depth to the magnetic sources in the survey area by setting an appropriate Structural Index, SI. The gridding interval enables recognition of any anomaly that is up to 75 m in wavelength, hence many solution points. A total of 34,595 solution points were obtained. Result with tightest cluster around recognized sources is likely to give the best solution and therefore accepted. However, obtained solution (Figure 15) was windowed to select the most accurate results. These solutions were obtained for varying SI values of 0, 1, and 2 with an average error in depth estimation less than the required maximum 11% tolerance and window size, and the result with the least unreal solutions was adopted. It was observed that for SI = 1 (i.e. dike model) was the best fit (Figure 15). The solution produced realistic results which were consistent with the type of geologic model of the study area. Solutions above the error tolerance levels were rejected.

Maximum depth limit was set to 250 m, horizontal uncertainty greater than 10% was rejected, and offset limit in *x* and *y* directions were likewise set to maximum of 5%.

The windowed Euler deconvolution solution points (Figure 16) coincides weakly with regions having high analytic signal amplitude and therefore likely to represent regions with meaningful anomalies and they are in dikes. Euler depth gave useful information about the subsurface topography of the basement complex. The windowed Euler depth solutions has color coded circles, the circle's colors indicate depth range and the size defines depth variation within the range.

Euler depths result ranged from 1 to 2233.9 m (Table 2) coinciding with rocks contacts while depth ranging between 0 and 132.2 m bsl correspond to part of the study area where the basement rocks are overlain by clastic materials. Solutions for Ado-Ekiti Southwest regions indicate relatively deep basement source, greater than 2000 m in depth bsl as seen underlying Ilawe Ekiti and progressively gets shallower northwards and southwards. The Euler depth below the datum are scattered all over the study area and are less conspicuous. Integrating the windowed Euler solution map with the proposed geologic map indicates that these magnetic sources align with lineaments and folds which play host to these dike bodies. Communities such as Iyin-ekiti (600-1000 m), Ilawe-Ekiti (1500-2200 m), parts of Ogotun Forest Reserve (250-750 m), Igbara-Odo (0 to 100 m and 0 to 1500 m) indicating negative and positive anomalies respectively, Erijiyan (750-1500 m) and Apata Hill (250-1000 m) all correspond to part of the study area underlain by lineaments and folds which host these sources. These communities fall under the basement terrain with visible basement rocks exposures. The region has varied source depth solutions from approximately 100 m to 2200 m.

Conclusion

Airborne magnetic datasets over the area were collected, processed, and enhanced in order to map the lithology and geological structures of the study area. Filtering techniques of aeromagnetic method were used to enhance the dataset; the residual magnetic intensity (RMI) was filtered using reduction to the equator (RTE), analytic signal, first order vertical and horizontal derivatives, tilt derivative (TDR) and upward continuation (UC). These filters helped define the lithological boundaries, intersection of geological structures, faults, folds, sheared zones, and contacts. The tilt derivative (TDR) was very useful for the delineating most of geological structures in the area and in detecting that the rocks are striking northeast-southwest generally in accordance with the major structural trend of the basement complex of Nigeria as observed from several earlier works by Ojo (1990) and Ako et al., (2004). The depth to the magnetic sources within the study area was determined using both average redial power spectrum and Euler deconvolution depth estimation methods. The power spectrum produced shallow depth range of 360 m to 1350 m while the Euler deconvolution which was associated with dikes on the other hand produced deeper depth range of 100 m to 2200 m and this dike structural index best fits the study area. This is because dikes anomaly generally occur at great depth.

Acknowledgements

The authors wish to profoundly appreciate the Nigeria Geological Survey Agency for the release of the aeromagnetic data.

References Cited

Ajakaiye, D.E., D.H. Hall, J.A. Ashieka, and E.E. Udensi, 1991, Magnetic Anomalies in the Nigerian Continental Mass based on Aeromagnetic Surveys, *in* P. Wasilewski and P. Hood (Eds.), Magnetic Anomalies-Land and Sea: Tectonophysics, v. 192, p. 211-230.

Ako, B.D., S.B. Ojo, C.S. Okereke, F.C. Fieerge, T.R. Ajayi, A.A. Adepelumi, J.F. Afolayan, O. Afolabi, and H.O. Ogunwusi, 2004, Some Observations from Gravity/Magnetic Data Interpretation of the Niger Delta: NAPE bulletin, v. 17, p. 11-21.

Alexander, M., J.C. Pratsch, and P. Corine, 1998, Under the Northern Gulf Basin: Basement Depths and Trends: Abstract, Society of Exploration Geophysicists Sixty-Eight Annual Meeting, New. Orleans, LA, p. 45-49.

Ball, E., 1980, An Example of very Consistent Brittle Deformation over a Wide Intra-continental Area: The Late Pan-African Fracture System of the Tuareg and Nigerian Shield: Tectonophysics, v. 61, p. 363–379.

Baranov, V., 1957, A New Method for Interpretation of Aeromagnetic Maps Pseudo-Gravimetric Anomalies: Geophysics, v. 22, p. 359-383.

Barbosa, V.C.F., J.B.C. Silva, and W.E. Medeiros, 2000, Making Euler Deconvolution Applicable to Small Ground Magnetic Surveys: Journal of Applied Geophysics, v. 43, p. 55–68.

Blakely, R.J., 1995, Potential Theory in Gravity and Magnetic Applications: Cambridge University Press, Cambridge, 441 p.

Blanco-Montenegro, I., J.M. Torta, A. García, and V. Araña, 2003, Analysis and modelling of the aeromagnetic anomalies of Gran Canaria (Canary Islands): Earth Planet. Sci. Lett., v. 206, p. 601–616.

Briggs, I.C., 1974, Machine Contouring Using Minimum Curvature: Geophysics, v. 39, p. 39–48.

Dobrin, M., and C. Savit, 1988, Introduction to Geophysical Prospecting: McGraw-Hill, NY, 867 p.

El Dawi, M.G., L. Tianyou, S. Hui, and L. Dapeng, 2004, Depth Estimation of 2-D Magnetic Anomalous Sources by using Euler Deconvolution Method: American Journal of Applied Sciences, v. 1/3, p. 209–214.

Feumoe, A.N., T. Ndougsa-Mbarga, E. Manguelle-Dicoum, and J.D. Fairhead, 2012, Delineation of Tectonic Lineaments Using Aeromagnetic Data for the South-East Cameroon Area: Geofizika, v. 29, p 175-192.

Graham, K.M., K. Preko, D.D. Wemegah, and D. Boamah, 2014, Geological and Structural Interpretation of part of the Buem Formation, Ghana, Using Aerogeophysical Data: Journal of Environment and Earth Science, v. 4/4, p. 17-31.

Kivior, I., and D. Boyd, 1998, Interpretation of the Aeromagnetic Experimental Survey in the Eromanga/Cooper Basin: Can. J. Explor. Geophys, v. 34/1-2, p. 58-66.

McMurry, P., 1976, The Geology of the Precambrian to Lower Paleozoic Rocks of Northern Nigeria - A Review, *in* C.A. Kogbe (ed.), Geology of Nigeria, Elizabethan Press, Lagos, p. 15-39.

Muszala, S.P., N.R. Grindlay, and R.T. Bird, 1999, Three-dimensional Euler Deconvolution and Tectonic Interpretation of Marine Magnetic Anomaly Data in the Puerto Rico Trench: Journal of Geophysical Research, v. 104/B12, p. 29,175-29,187.

Ndougsa-Mbarga, T., A.N.S. Feumoe, E. Manguelle-Dicoum, and J.D. Fairhead, 2011, Aeromagnetic Data Interpretation to Locate Buried Faults in South-East Cameroon: Geophysical Society of Finland, Helsinki, 63 p.

Nettleton, L.L., 1971, Elementary Gravity and Magnetics for Geologists and Seismologists: Society of Exploration Geophysicists, Tulsa, 121 p.

Odeyemi, I., 1981, A Review of the Orogenic Events in the Precambrian Basement of Nigeria, West Africa: Geologische Rundschau, v. 70, p. 897-909.

Ojo, S.B., 1990, Origin of a Major Magnetic Anomaly in the Middle Niger Basin, Nigeria: Tectonophysics, v. 185, p. 153-162.

Olanrewaju, V.O., 1981, Geochemistry of Charnockite and Granite Rocks of the Basement Complex around Ado-Ekiti – Akure, Southwest, Nigeria: PhD Thesis, University of London, London.

Osinowo, O.O., and A.I. Olayinka, 2013, Aeromagnetic Mapping of Basement Topography around the Ijebu-Ode Geological Transition Zone, Southwestern Nigeria: Acta Geodaetica et Geophysica., v. 48/3, p. 451-470.

Oversby, V.M, 1975, Lead Isotope Study of Aplites from the Precambrian Basement Rocks near Ibadan, Southwestern Nigeria: Earth Planets. Sci. Lett., v. 27, p. 177 – 180.

Peterson, N.V., E.A. Groh, E.M. Taylor, and D.E. Stensland, 1976, Geology and Mineral Resources of Deschutes County Oregon: Oregon Department of Geology and Mineral Industries Bulletin, v. 89, p. 1-62.

Phillips, J.D., R.W. Saltus, and R.L. Reynolds, 1998, Sources of Magnetic Anomalies Over a Sedimentary Basin - Preliminary Results from the Coastal Plain of the Arctic National Wildlife Refuge, Alaska, *in* R.I. Gibson and P.S. Millegan (eds.), Geologic Applications of Gravity and Magnetics: Case Histories: Society of Exploration Geophysicists and American Association of Petroleum Geologists, p.130-134.

Pratt, D.A., and Z. Shi, 2004, An Improved Pseudo-Gravity Magnetic Transform Technique for Investigation of Deep Magnetic Source Rocks: ASEG 17th Geophysical Conference and Exhibition, Sydney, p. 1-4.

Reid, A.B., J.M. Allsop, H. Granser, A.J. Millett, and I.W. Somerton, 1990, Magnetic Interpretation in Three Dimensions Using Euler Deconvolution: Geophysics, v 55, p 80-91.

Roy, L., B.N.P. Agarwal, and R.K. Shaw, 2000, A New Concept in Euler Deconvolution of Isolated Gravity Anomalies: Geophysical Prospecting, v. 48/3, p. 559-575.

Spector, A., and F. Grant, 1970, Statistical Models for Interpreting Aeromagnetic Data: Geophysics, v. 35, p. 293-302.

Talabi, A.O., 2013, Hydrogeochemistry and Stable Isotopes (δ18O and δ2H) Assessment of Ikogosi Spring Waters: American Journal of Water Resources, v. 1/3, p. 25-33.

Telford, W.M, L.P. Geldart, R.E. Sheriff, and D.A. Keys, 1990, Applied Geophysics: Cambridge University Press, Cambridge, p. 792.

Thompson, D.T., 1982, EULDPH—A New Technique for Making Computer Assisted Depth Estimates from Magnetic Data: Geophysics, v 47, p 31-37.

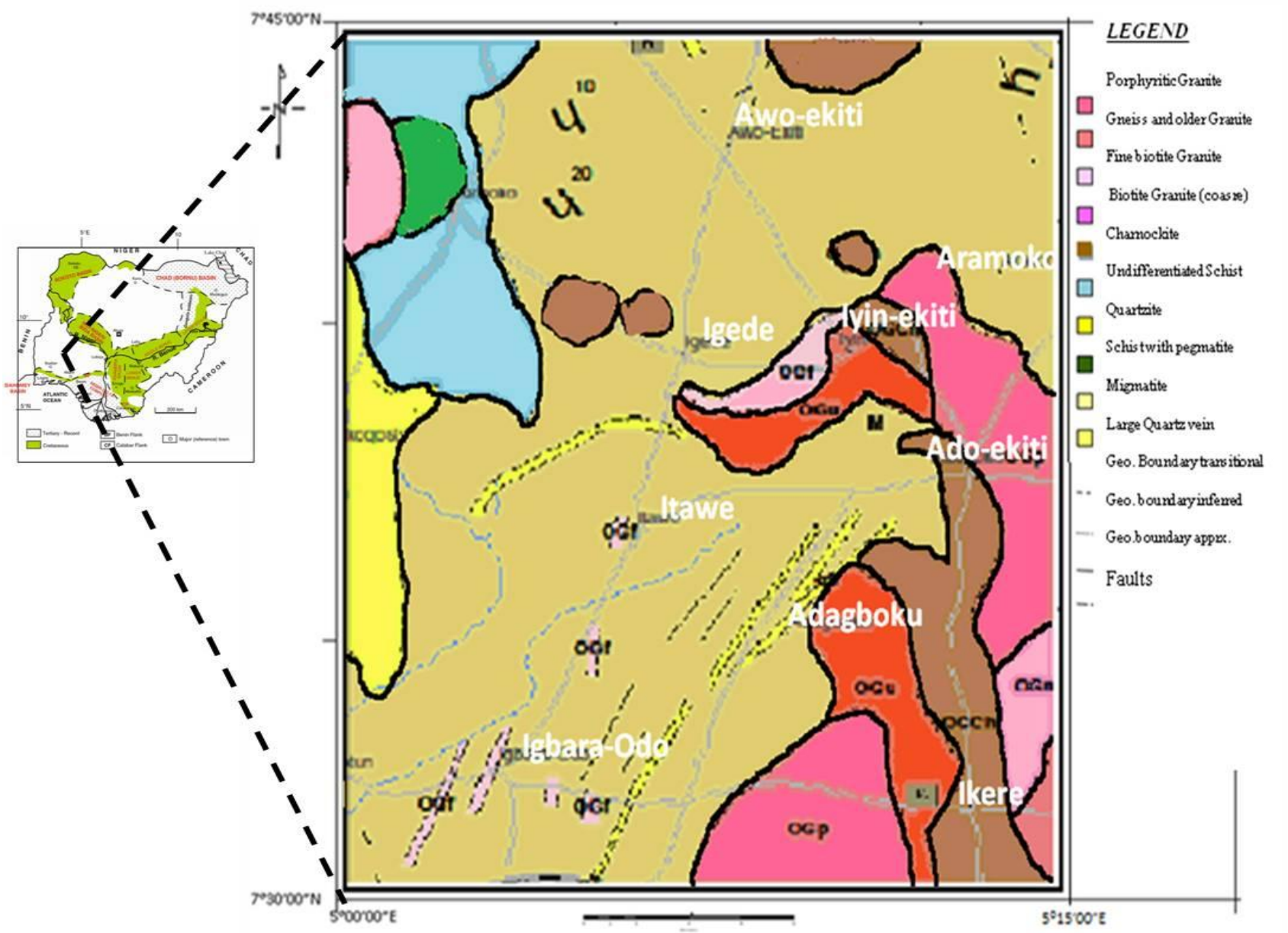

Figure 1. Geological map of Ado-Ekiti Southwest (source: Nigeria Geological Survey Agency).

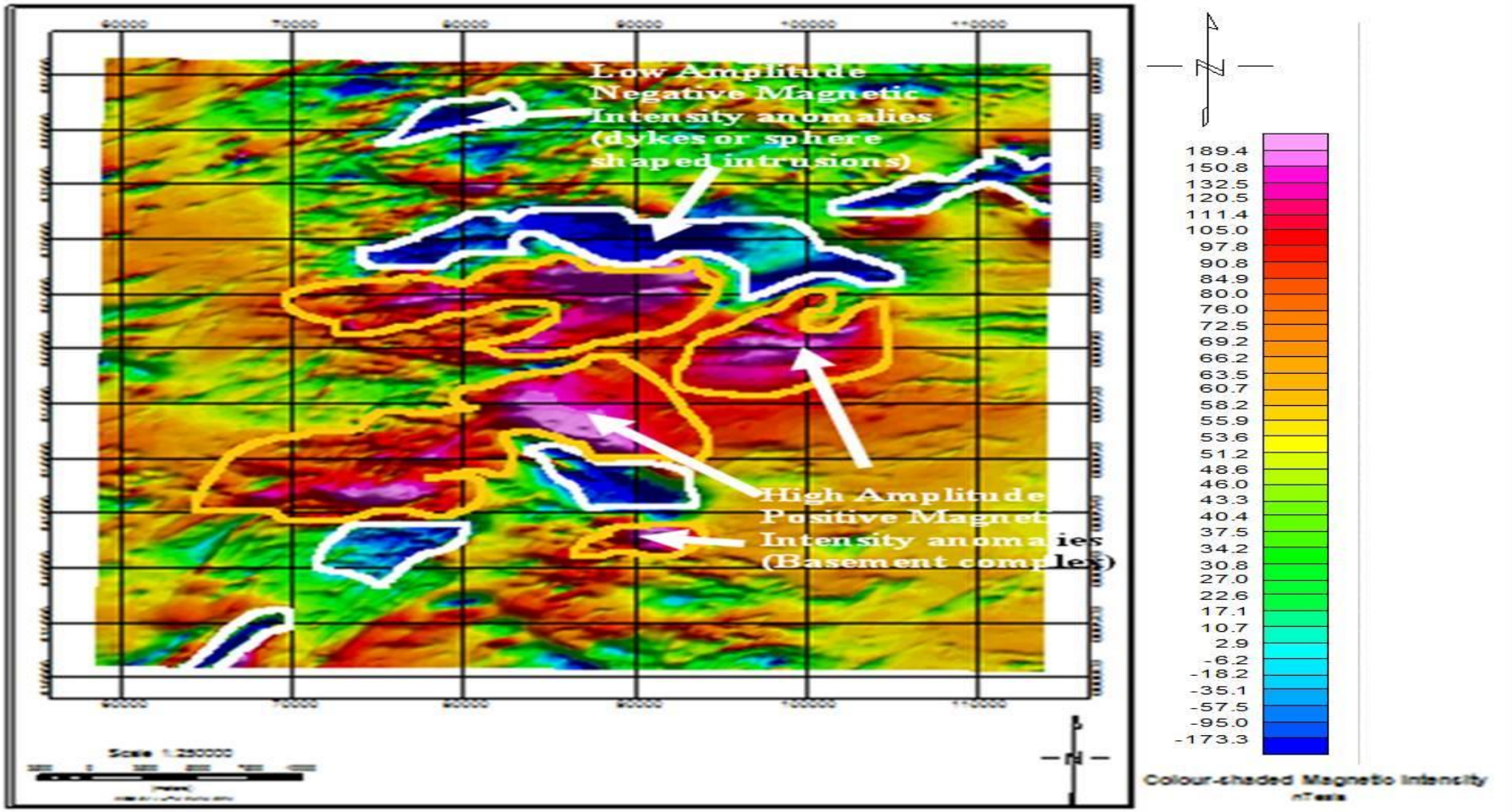

Figure 2. Color shaded total magnetic intensity map of Ado-Ekiti Southwest and environs.

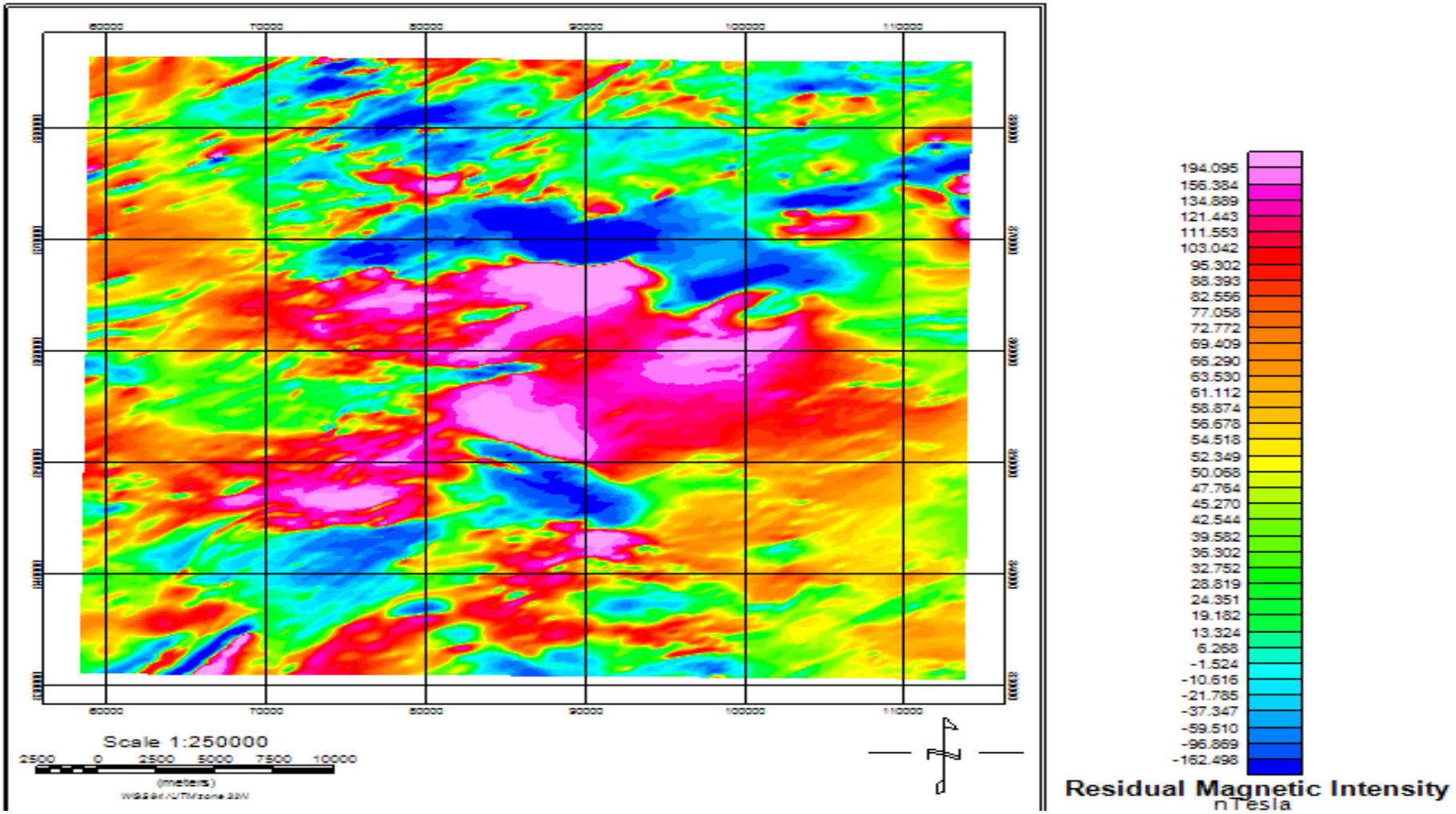

Figure 3. Reduction to equator map of Ado-Ekiti Southwest and environs.

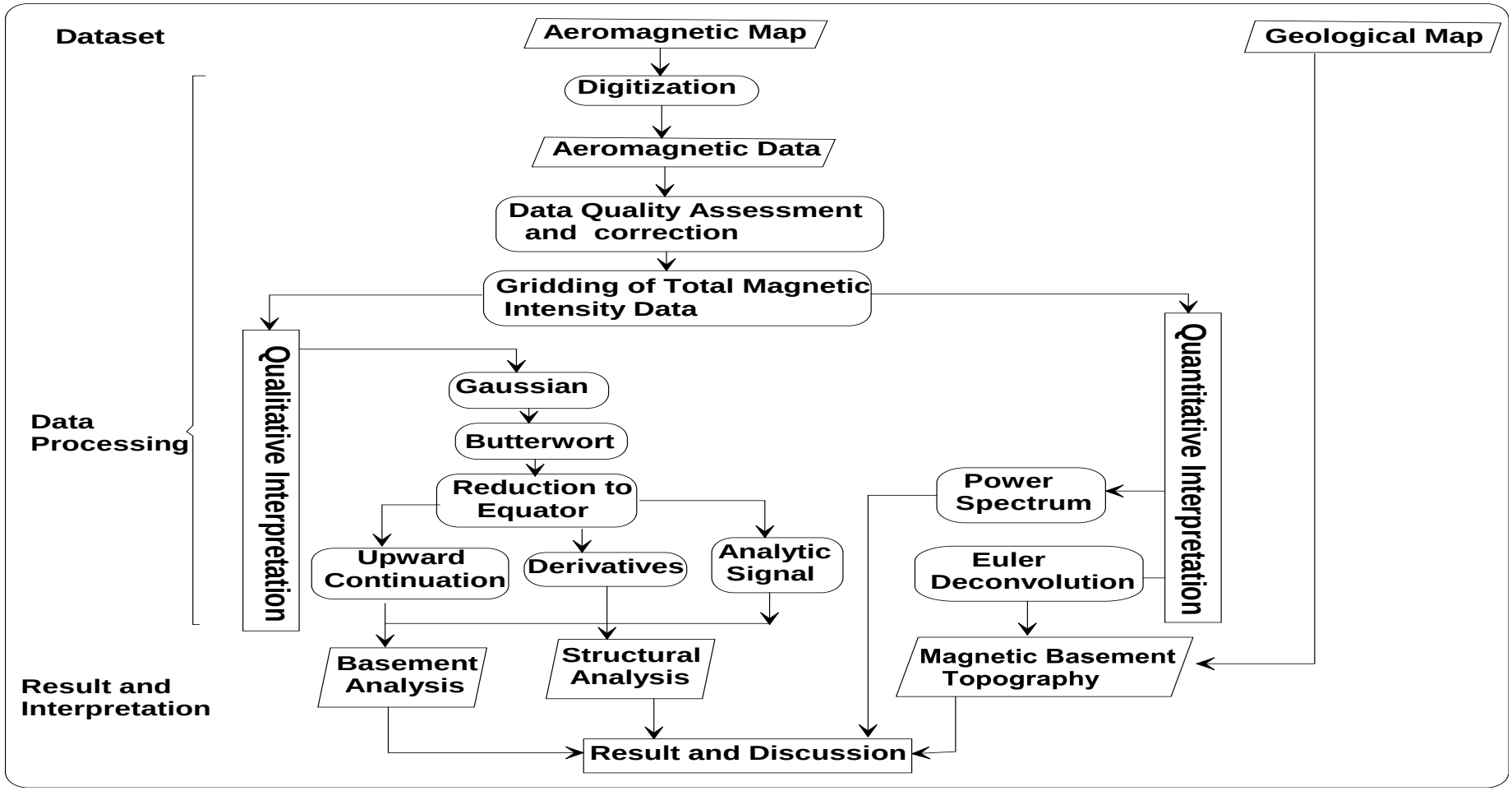

Figure 4. Research Methodology Flow Chart.

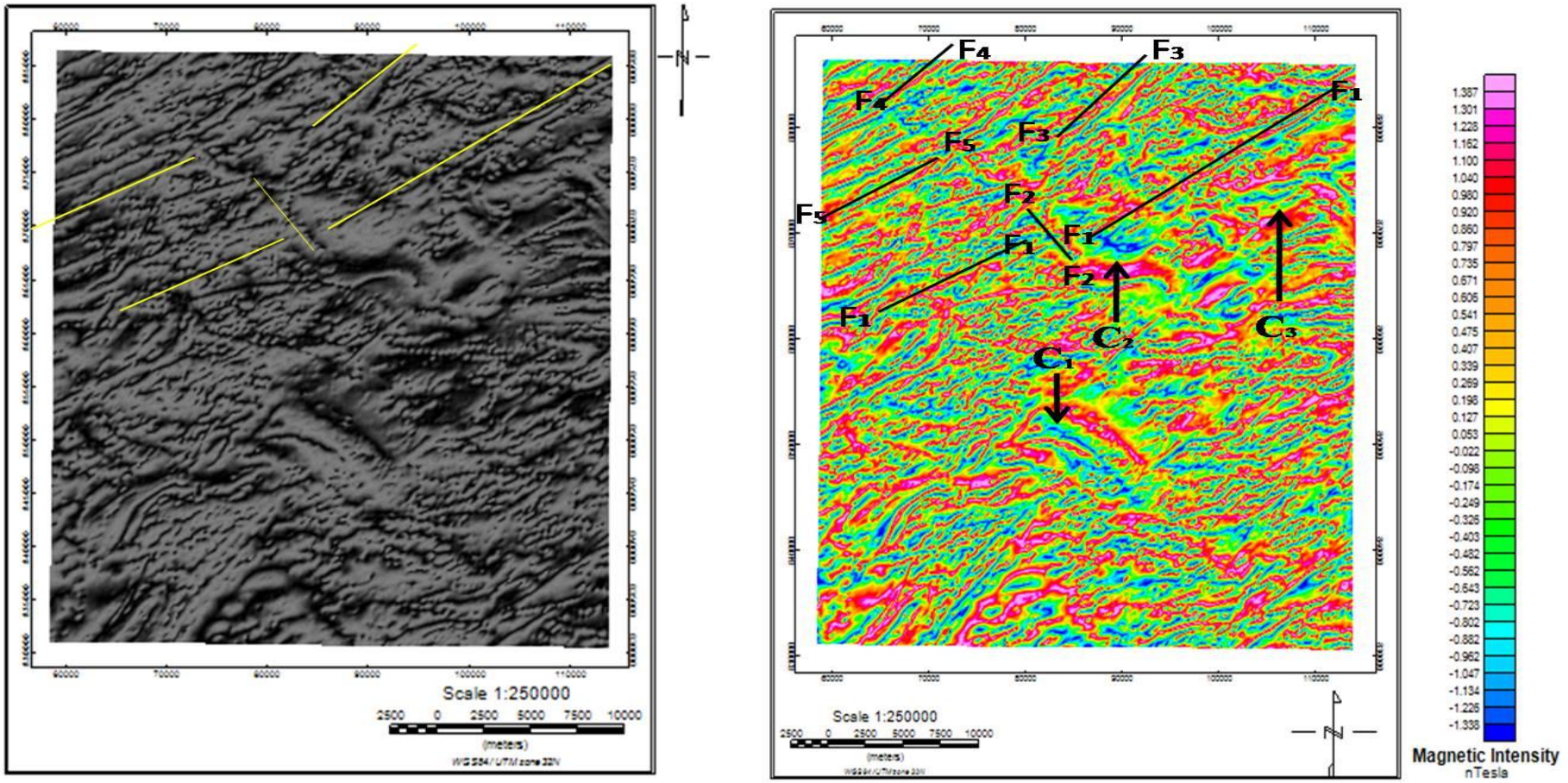

Figure 5. A. Grey shaded tilt derivative map. B. Color shaded tild derivative map of the study area.

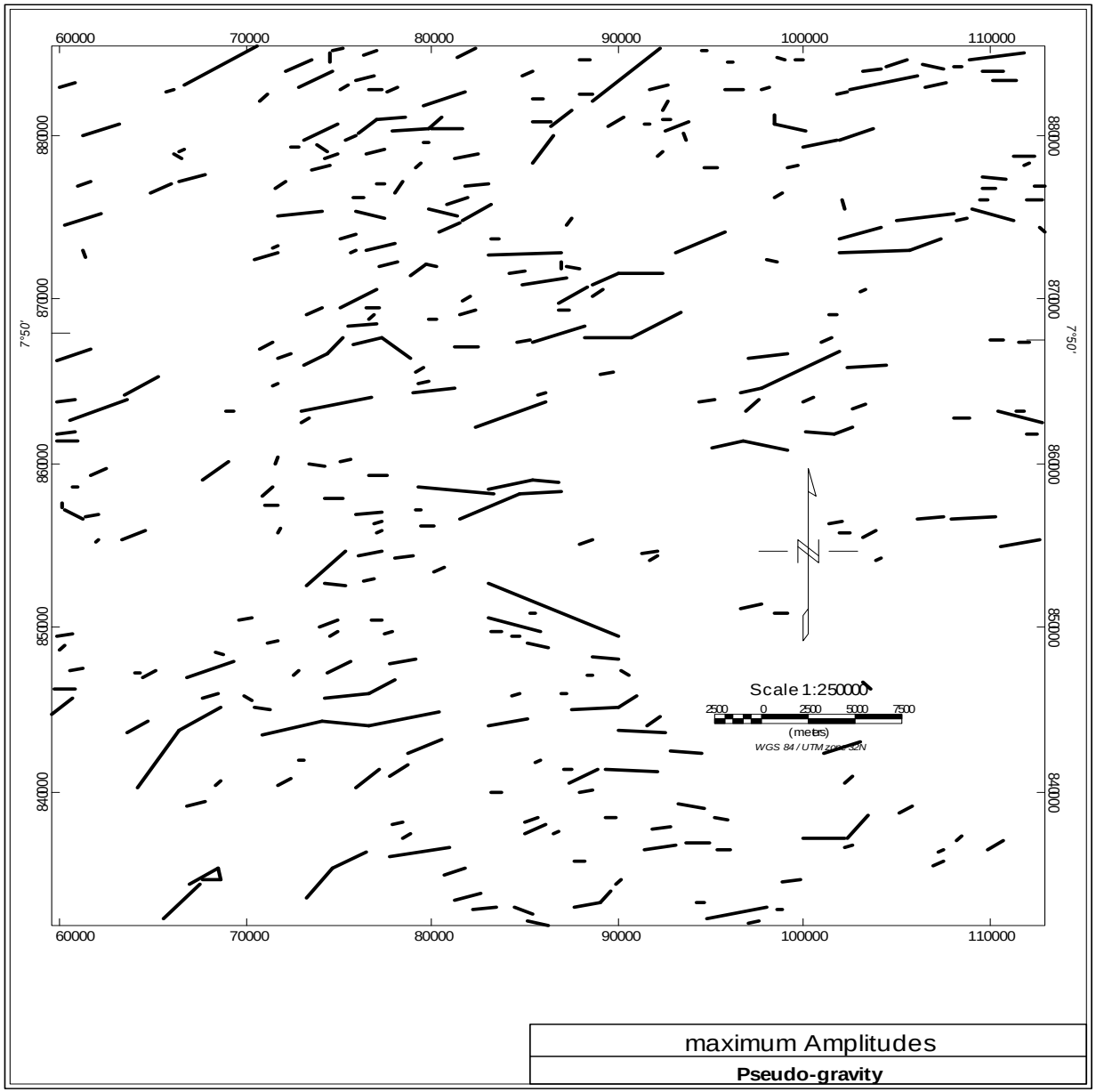

Figure 6. Lineaments and archs marked out by Vectorisation.

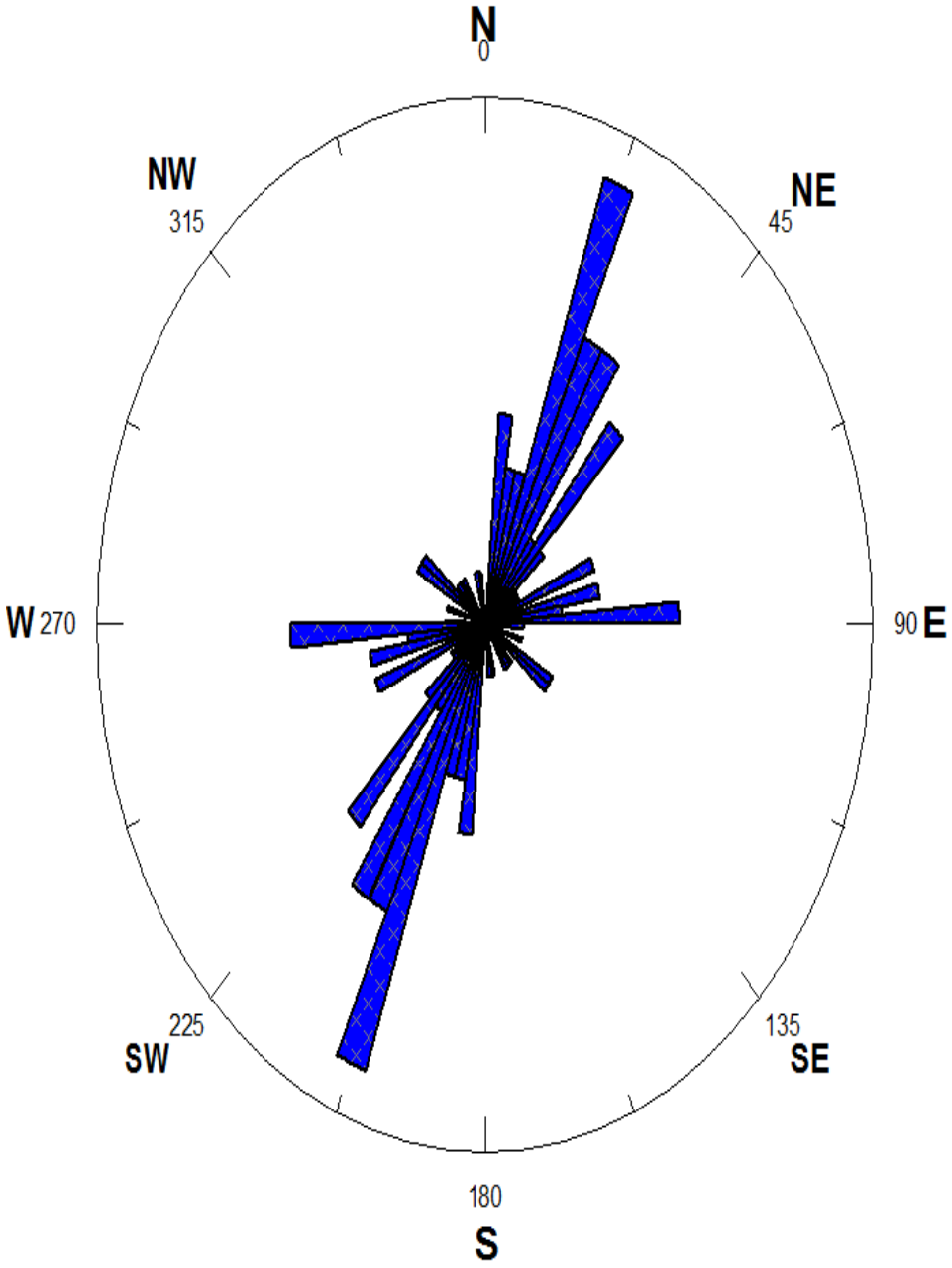

Figure 7. Rose diagram of the lineaments.

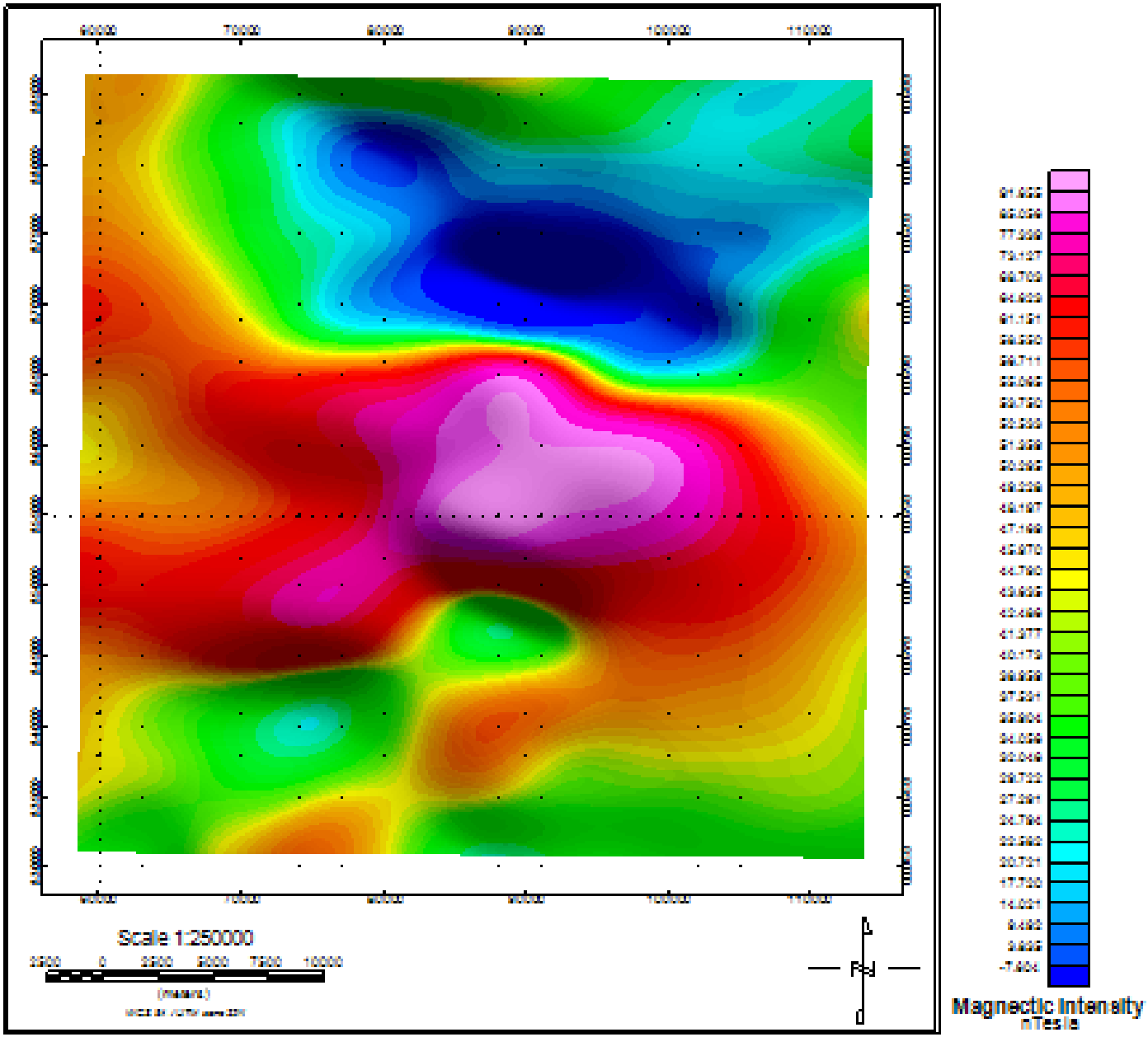

Figure 8. Upward continuation map of Ado-Ekiti Southwest and environs.

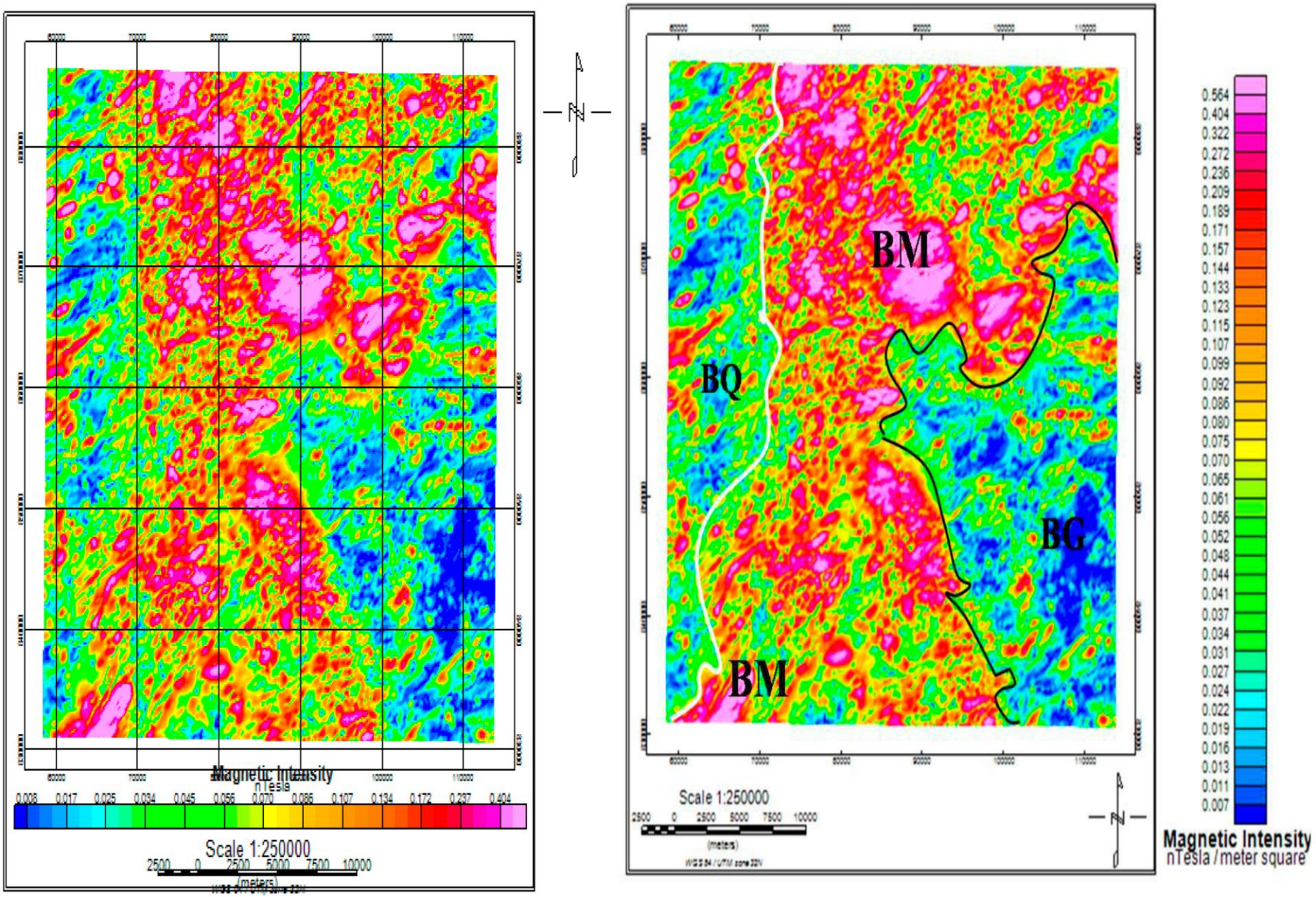

Figure 9. Analytical Signal of Ado-Ekiti Southwest, sheet 244.

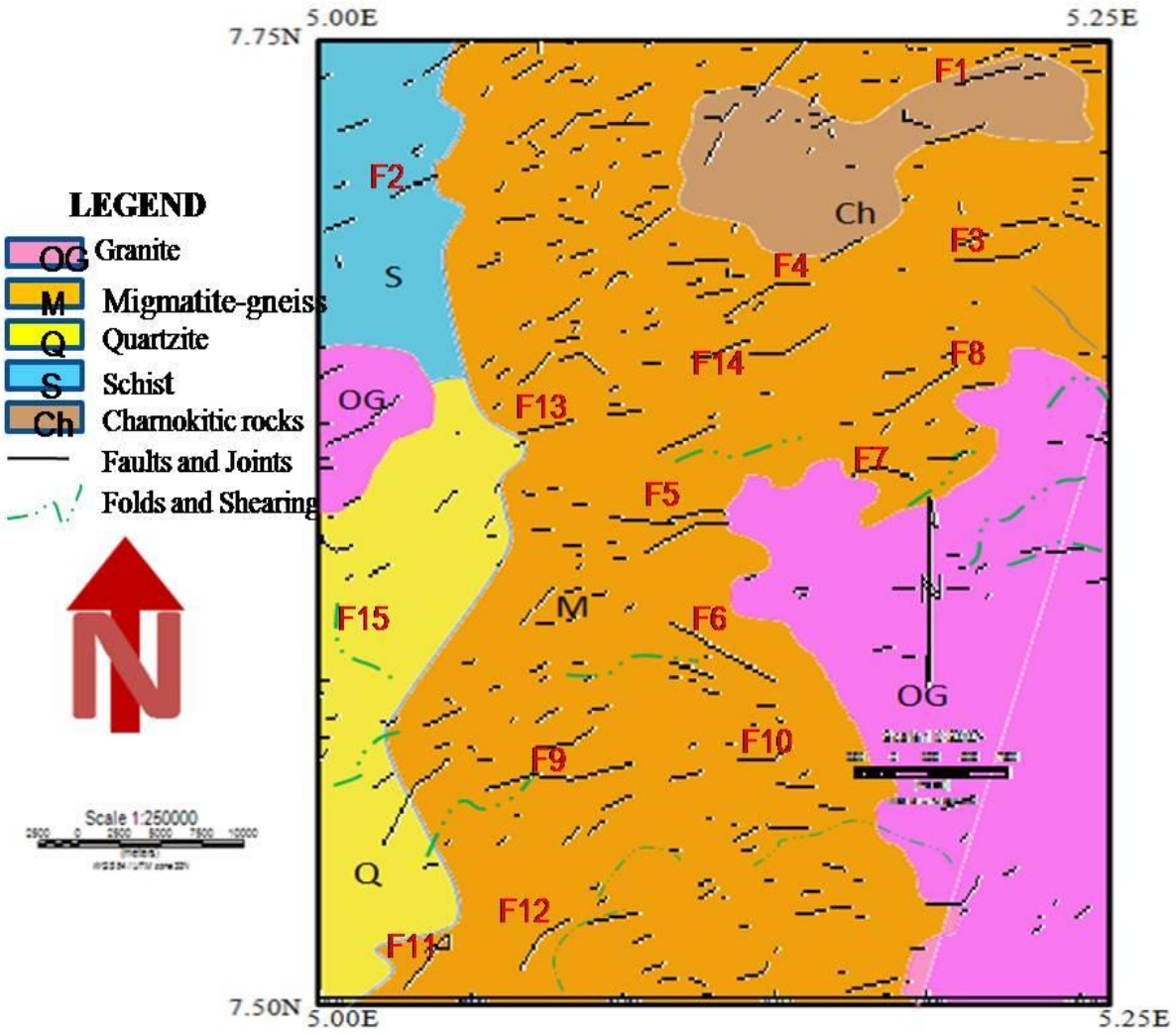

Fault segment	Dip	Depth (m)
F1	ENE	500
F2	ENE-SWS	300
F3	vertical	1000
F4	SW-NE	500
F5	vertical	2000
F6	NW-SE	1700
F7	vertical	550
F8	NNE-SSW	650
F9	vertical	750
F10	vertical	500
F11	SW-NE	750
F12	SW-NE	500
F13	vertical	450
F14	vertical	1600
F15	N-S	100

Figure 10. Proposed geologic map of the area aligned with faults and their relative depths of occurrence.

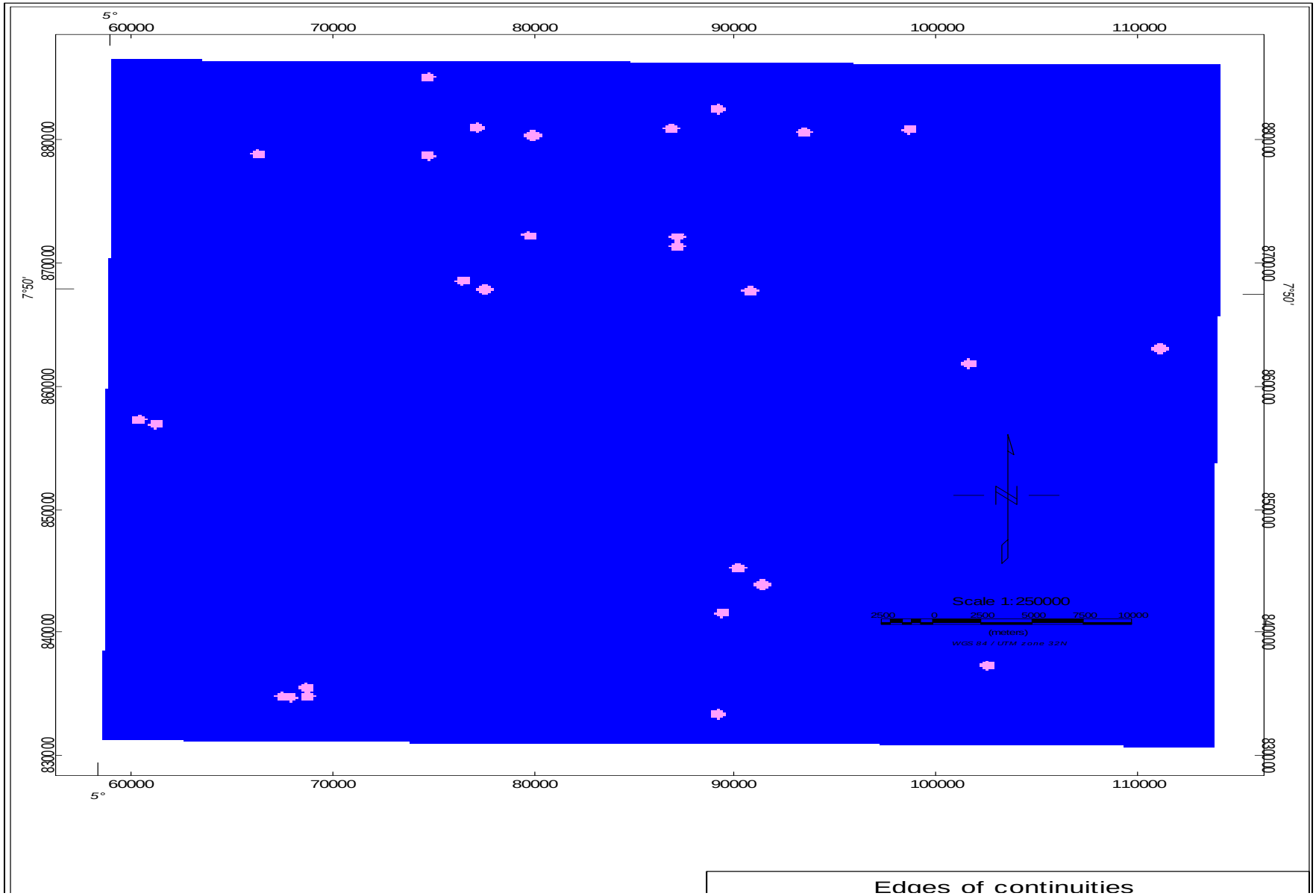

Figure 11. Contact occurrence density.

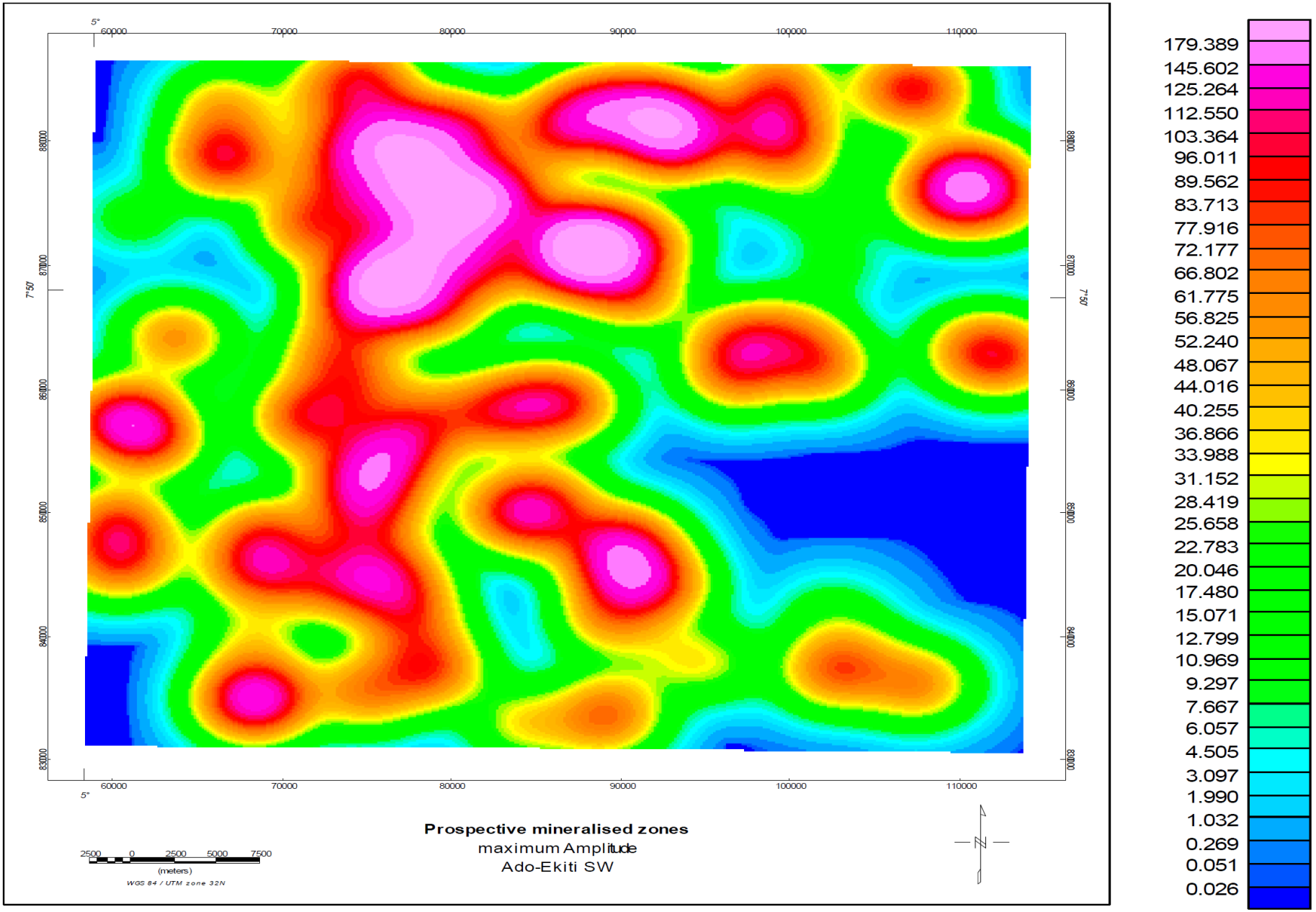

Figure 12. Orientation entropy heat map indicating mineralization zone.

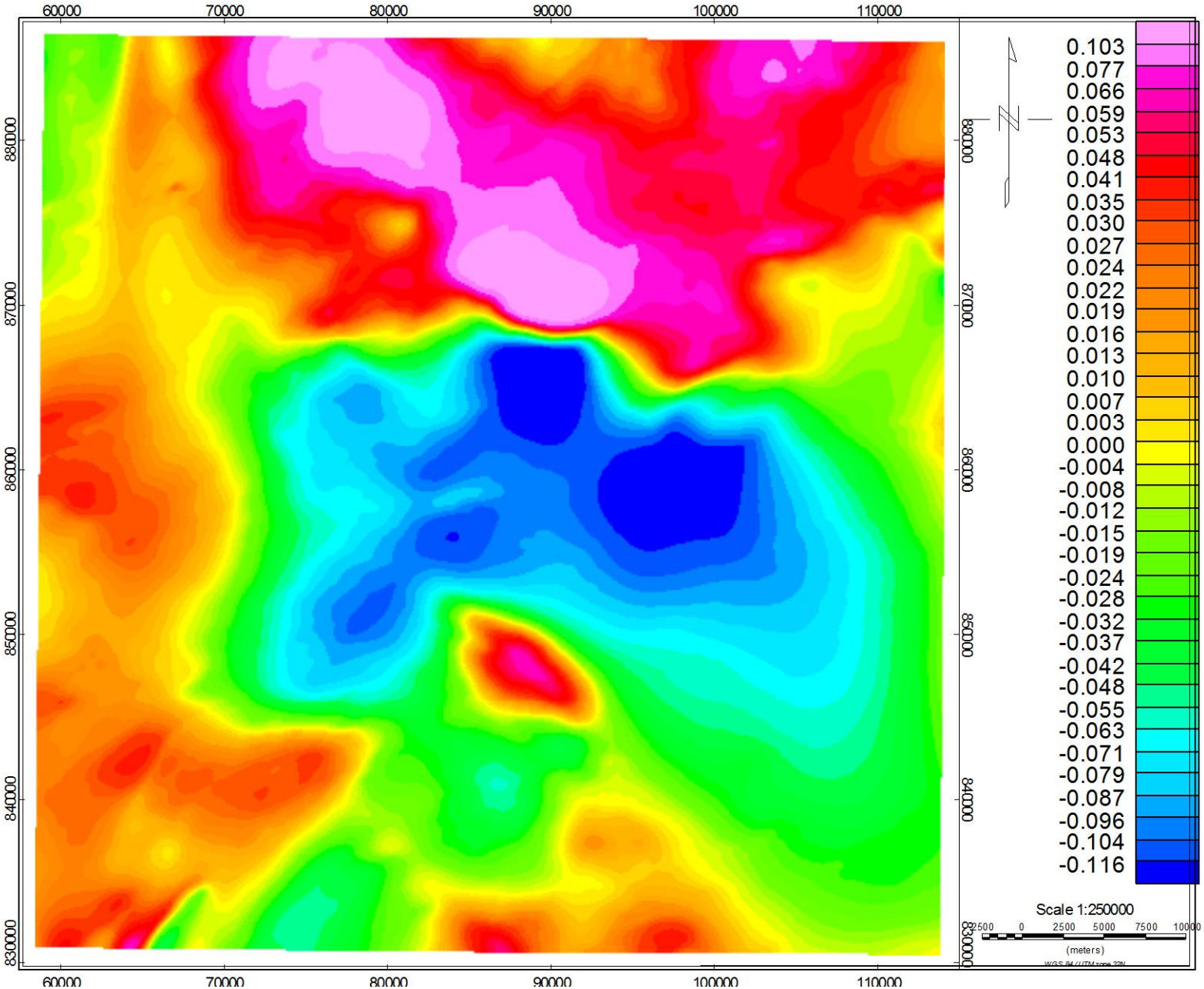

Figure 13. Psuedo-gravity map of the study area.

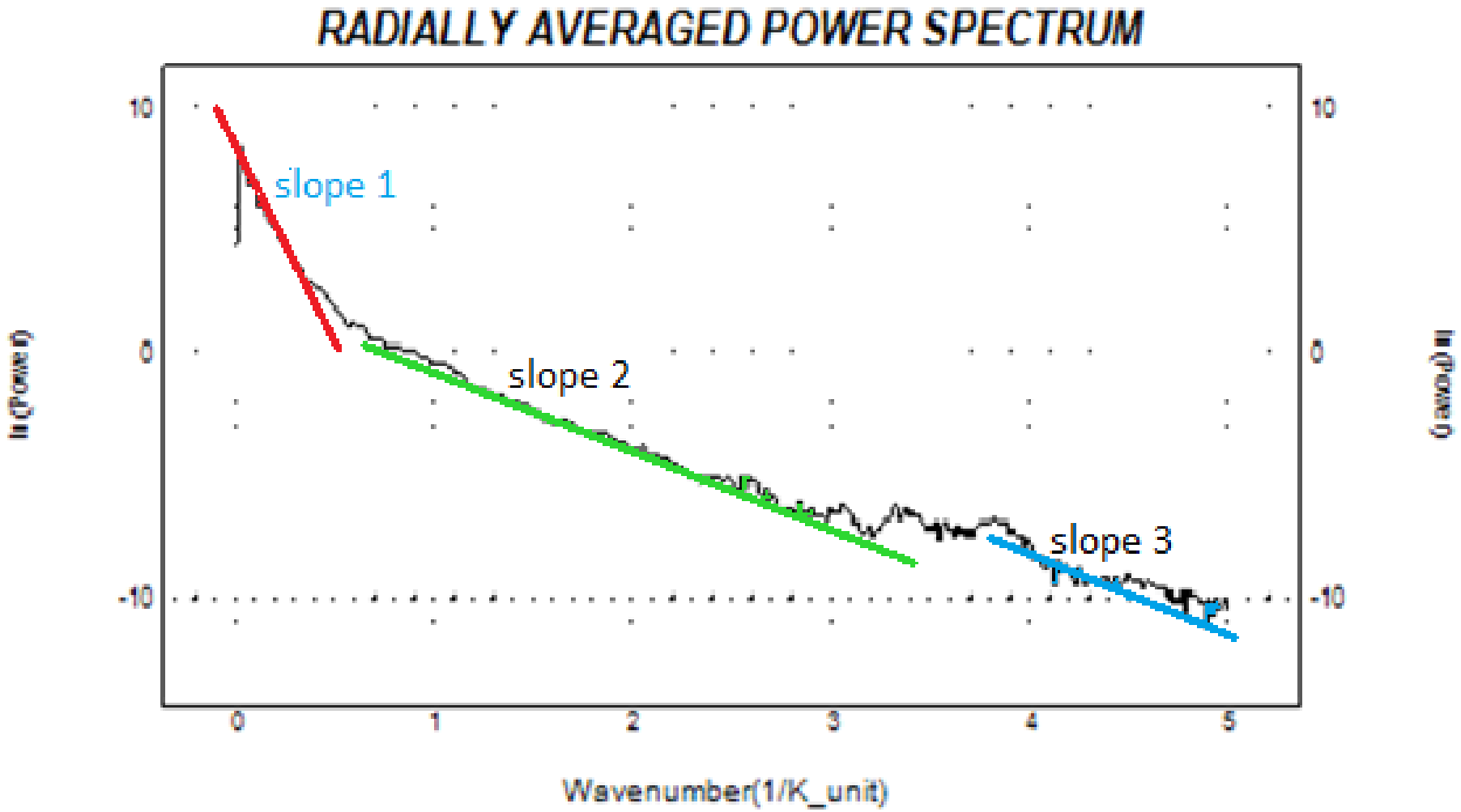

Figure 14. Average power spectrums of aeromagnetic anomaly map indicating gradients used in calculating the average depth to the top of magnetic sources.

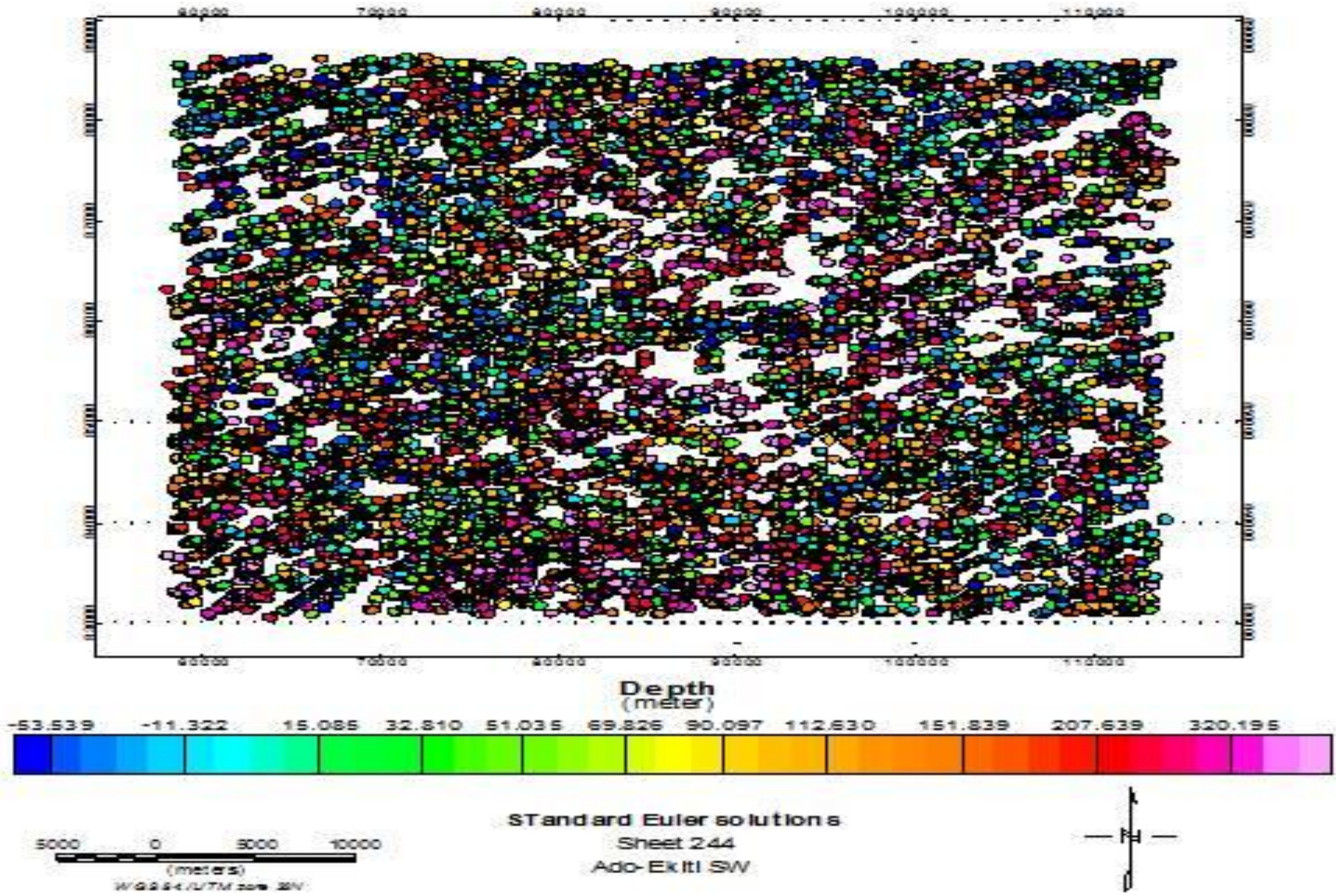

Figure 15: Standard Euler solutions of Ado-Ekiti Southwest and its adjoining areas.

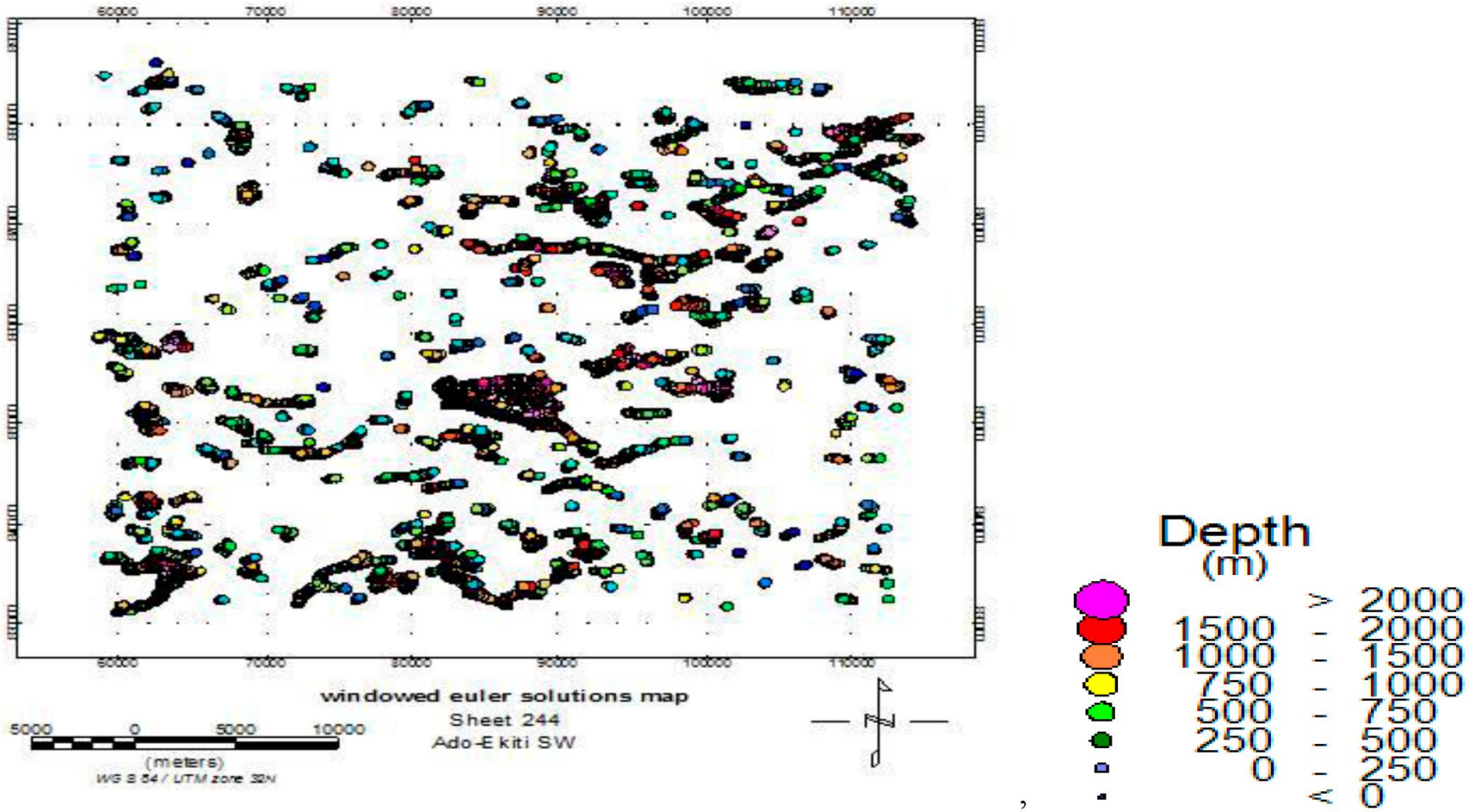

Figure 16. Windowed Euler solution map of Ado-Ekiti Southwest and its adjoining areas.

Structural Index, η	Type of magnetic model	Characteristics
0.0	Contact with large extent	Circles are intertwined with no particular pattern
0.5	Contact with small extent	Circles are intertwined in a pattern that is linear and in rows
1.0	Sills and dyke, Thin prism with large circles	Circles are intertwined in a straight line
2.0	Vertical and horizontal cylinder	Occurs like a vertical pipe and Circles intertwined neatly with regular circumference
3.0	Sphere	Occur has sphere bodies of circles with a common axis connecting them.

Table 1. The following table summarizes the structural indices for simple models in a magnetic field.

Statistics Information	Depth To Source (m)
Minimum depth value:	132.2
Maximum depth value	2233.9
Mean value	213.6
Standard deviation	142.7
Arithmetic sum	3930483.8

Table 2. Table showing the statistical report of the results of depth obtained.